Optimization of the Injector Spray Angle of a 4-Stroke Natural Gas-Diesel DF Marine Engine

Pham Van Chien
Interdisciplinary Major of Maritime AI Convergence
Korea Maritime and Ocean University
Busan, Korea

Maritime Academy
Ho Chi Minh City University of Transport
Ho Chi Minh City, Vietnam
chien.pham@ut.edu.vn

Le Van Vang
Maritime Academy
Ho Chi Minh City University of Transport
Ho Chi Minh City, Vietnam
levanvang@ut.edu.vn

Ngo Duy Nam
Maritime Academy
Ho Chi Minh City University of Transport
Ho Chi Minh City, Vietnam
nam.ngo@ut.edu.vn

Lee Won-Ju
Division of Marine System Engineering
Korea Maritime and Ocean University
Busan, Korea
skywonju@kmou.ac.kr

Choi Jae-Hyuk
Division of Marine System Engineering
Korea Maritime and Ocean University
Busan, South Korea
choi_jh@kmou.ac.kr

***Abstract*— This work studied the effect of injector spray angle on the combustion process and emission characteristics of a 4-stroke port-injection Natural Gas-Diesel dual-fuel marine engine to determine the optimal spray angle for the fuel injector aiming to reduce exhaust gas emissions while keeping engine performance. Three-dimensional simulations of the combustion and emission formations occurring inside the cylinder of the engine operating in both diesel and DF modes were carried out using the AVL FIRE code. The engine's in-cylinder temperature, pressure, and emission characteristics were analyzed. To clarify the effect of the injector spray angle on the combustion and emission characteristics of the engine, only injector spray angle has been varied from 145 to 160 º. In contrast, all other boundary conditions and working conditions of the engine have remained unchanged. The simulation results have been compared and showed good agreement with the experimental results conducted in the researched engine. The study has successfully investigated the effects of fuel spray angle on the combustion and emission characteristics of the engine. A better spray angle for the fuel injector in order to reduce NO emissions (145 º) or soot and CO_2 emissions (150 º) while keeping engine power almost unchanged without the use of any exhaust gas post-treatment equipment has also been suggested.**

Keywords—Combustion, emission, spray angle, NG-Diesel engines, dual-fuel engine.

I. INTRODUCTION

To limit the impact of emissions from ships on human health and the Earth's environment, the marine emission regulations released by the International Maritime Organization (IMO) are becoming stricter. As a result, emission reduction solutions are mandatorily applied on both new-building and existing ships nowadays to meet stricter emission regulations [1]-[3]. According to the MARPOL (International Convention for the Prevention of Pollution from Ships) Annex VI, since January 1st, 2020, all ships must comply with the use of fuel containing a maximum of 0.5% sulfur globally. The minimum reduction in carbon (C) intensity per marine transport means must be at least 40% by 2030 compared with 2008, with a target of at least 70% by 2050. Greenhouse gas (GHG) from ships by 2050 must be reduced by at least 50% compared to 2008. Since 2016, NOx emissions from ships have been limited to 3.4 g/kWh for engines with speeds less than or equal to 130 rpm (revolution per minute). This limitation gradually decreases with increasing engine speed and reaches only 2 g/kWh for engines with a speed higher than or equal to 2000 rpm [4]. There are various solutions for reducing emissions from marine engines, but this paper focuses on two aspects: fuel injection technologies and alternative fuels.

Among many kinds of fuels, NG which principally consists of methane (CH_4), has been and will still be widely used in heavy duty marine engines. It has many advantages, such as low EGEs, no processing, low price, abundant reserves, etc. However, since NG has a low cetane number (high auto-ignition temperature), it needs an external energy source for ignition, such as a spark plug in spark-ignition (SI) engines or pilot fuel (diesel oil) in DF engines. If NG is used in DF engines, pure diesel engines can be modified to an NG–diesel DF engine very easily and with only a low cost [5]-[7]. The detailed properties, as well as the effect of NG on the combustion and emission characteristics of an

NG–diesel DF marine engine, can be found in our previous studies [8], [9].

In internal combustion engines (ICEs), all the injected fuel should be in contact with all the oxygen (O_2) available in the combustion chamber so that the fuel combustion can take place as completely as possible. Both the fuel atomization and injection characteristics are the major factors in reducing EGEs while keeping or even enhancing engine power [10]. Regarding the fuel injection characteristics, injection method (port-injection or direct-injection), injection strategy (single-injection or multiple-injection), injection timing, and spray angle (SA) play important roles in the combustion and emission characteristics of direct injection (DI) engines [5], [6]. Injector SA has a strong influence on the combustion and emission formation of DI engines as it determines the fuel injection targeting point in the combustion chamber [11]. Therefore, studies for injector SA are very important and will have implications for both engine design and operating engineers. In this study, the effect of injector SA on the combustion and emission characteristics of a 4-stroke port-injection Natural Gas-Diesel dual-fuel (NG-Diesel DF) marine engine was investigated by using the CFD analysis. The combustion and emission formation occurring inside the engine cylinder were modeled by using the AVL FIRE code.

The ultimate target of this study was to specify the optimal injector SA for the engine. The CFD models were validated by the experimental results reported in the engine's shop test technical data. The study also successfully assigned the optimal injector SA for the engine to achieve certain emission reductions.

II. NUMERICAL ANALYSIS

A. Engine Specifications

Figure 1 presents the schematic diagram of the engine in this study. The piston surface of the engine had a ω-type shape. The nozzle for pilot fuel injection has 12 identical holes with a designed SA of 155. The specification of the engine is presented in table I.

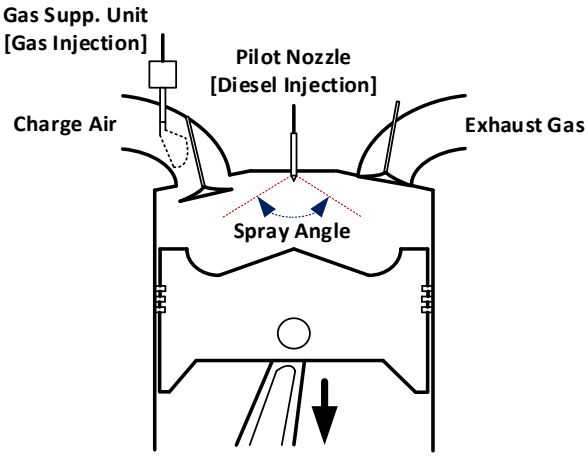

Figure 1. Schematic of the researched engine.

TABLE I. ENGINE SPECIFICATION.

Parameter	Value	Unit
Engine Type	4-Stroke DF Engine	
No. of Cylinder	6	
Fuel Gas Supplying	Port-Injection	
Ignition	Pilot Fuel	
Cylinder Bore x Stroke	350 x 400	mm
Compression Ratio	13.5:1	
MCR Speed	720	rpm
MCR Power	2880 @ 720 rpm	kW
IMEP	20	Bar

The engine can operate smoothly in two modes: diesel and DF mode. In the diesel mode, the engine works with pure diesel, as same as in conventional CI diesel engines. In the DF mode, NG serves as the primary fuel while diesel plays a role as the pilot fuel. In this mode, gas is injected into the intake port by a gas nozzle. It mixes with the charge air to form a premixed mixture prior to being supplied into the cylinder during the suction stroke of the engine. Whereas, the pilot fuel (diesel oil) is injected directly into the cylinder by a pilot nozzle mounted in the center of the engine cylinder cover.

In this study, $C_{13}H_{23}$ was employed to represent diesel oil. It acted as the pilot fuel to provide an ignition source for the premixed NG-air mixture. Whereas, methane (CH_4) was used to represent NG and acted as the primary fuel in the DF mode. All the fuel properties are temperature-dependence functions.

B. Computational Mesh, Boundary, and Initial Conditions

The Three-dimensional (3D) model of the combustion chamber and computational grid (mesh) for CFD analysis was built using the AVL FIRE ESE-Diesel platform. Owing to the axial symmetry characteristics of the combustion chamber; the pilot nozzle has 12 identical holes; and to reduce calculation time, only 1/12 of the entire 3D mesh of the combustion chamber was created. The calculation started from the intake valve closing (IVC) to the exhaust valve opening (EVO) and conducted in series using a twelve-core processor and took approximately 36 h of calculation time.

Figure 2 presents the computational mesh when the piston is at 40 crank angle degrees (CAD) after the top dead center (ATDC).

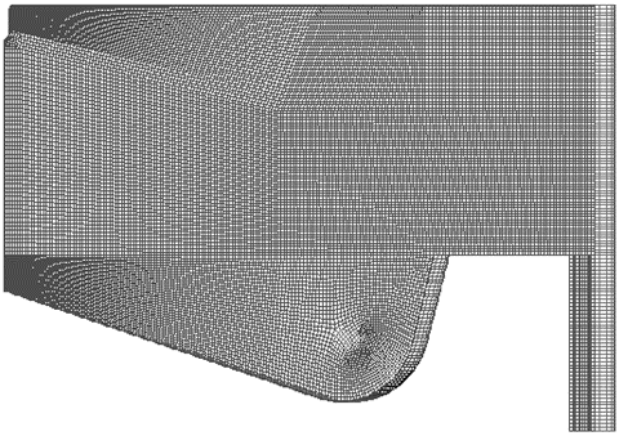

Figure 2. The computational mesh of the combustion chamber at 40 CAD ATDC.

The boundary and initial conditions for the CFD analysis were selected from the technical report of the researched engine and listed in table II.

TABLE II. BOUNDARY AND INITIAL CONDITIONS.

Boundary Conditions	**Boundary Type/ Specific Condition**
Piston surface	Mesh movement/Temp./97 °C
Cylinder liner	Wall/Temp./ 197 °C
Cylinder head	Wall/Temp./ 297 °C
Segment cut	Periodic
Initial Conditions	**Values**
Temperature at IVC	47 °C
Pressure at IVC	3.5 Bar
IVC	35 CAD ABDC
EVO	62 CAD BBDC
SOI	12 CAD BTDC
Pilot Injection Duration	7.5 milliseconds (Diesel mode)
	2.35 milliseconds (DF mode)

C. Simulation Cases

A total of eight simulations was performed for both diesel and DF modes. In each mode, the SA of the injector was changed from 145 to 160^o with an interval of 5^o. To clarify the effect of SA on the combustion and emission formation of the engine, only the SA of the injector was adjusted, while the other simulation parameters remained unchanged. The simulation cases in the present study are listed in table III.

TABLE III. SIMULATION CASES.

SA	**145 º**	**150 º**	**155 º**	**160 º**
Diesel Mode	Di-145	Di-150	Di-155	Di-160
DF Mode	DF-145	DF-150	DF-155	DF-160

D. CFD Models

The AVL FIRE software with its advanced models has been shown to be suitable for simulation the combustion process and emission formations inside the cylinder of diesel, gasoline and DF engines with very high accuracy [12]. In this study, the AVL FIRE ESE Diesel platform was used to model the working process of the engine from the IVC to the EVO. The

simulation results were then compared to the experimental results to validate the CFD models.

The k-ζ-f model was used to simulate the turbulence of the fluid flow inside the engine cylinder. This model has been developed from the k-ε two-equation turbulence model to become a four-equation model. It has higher accuracy and better stability than the original k–ε model [13]. In the CFD method, the transport and mixing process of chemical species in combustion problems are governed by solving equations of conservation that describe convection, diffusion phenomenon, concentrations for each component species, and reaction sources in the system. In this study, the extended coherent flame species transport model (ECFM) [14], [15] was utilized to simulate the combustion of fuels inside the engine cylinder. The direct injection process of the pilot fuel was modeled using the diesel nozzle flow model [15], [16]. This model offers a simple method to correct the velocity and initial diameters of fuel droplets owing to cavitation. The multi-component and WAVE models [15], [16] were used to simulate the evaporation and breaking up of fuel droplets, respectively. The self-ignition of diesel oil was simulated by the diesel ignited gas engine ignition model [15]. Regarding exhaust gas emissions, the extended Zeldovich mechanism [15], [17] was employed to model the NO formation inside the cylinder of the engine. It consists of seven species and three reactions and has been demonstrated to be able to predict the thermal NO emission in the cylinder of ICEs with high accuracy over a wide range of fuel-air equivalence ratios. The soot formation during the combustion process was modeled by the kinetic soot mechanism [15], [17]. The interaction between the combustion walls and fuel droplets was simulated by the Walljet1 model [15], [16]. Table IV summarizes the CFD models used in this study.

TABLE IV. CFD MODELS.

Model	Description	
Turbulence	k-ζ-f	
Combustion	ECFM	
Emissions	NO	Extended Zeldovich
	Soot	Kinetic Soot formation
Ignition	Diesel Mode	Auto-Ignition model
	DF Mode	Diesel Ignition Gas Engine model
Atomization	Breakup	WAVE
	Evaporation	Dukowicz model (Diesel Mode)
		Multi-component (DF Mode)
Droplet-Wall interaction	Walljet1	

E. CFD Model Validation

The CFD models were validated by comparing the simulation results to the experimental results reported in the shop test technical data of the engine. Figure 3 presents the comparisons between the simulation and experimental results for both diesel and DF modes in the original SA (155°) case.

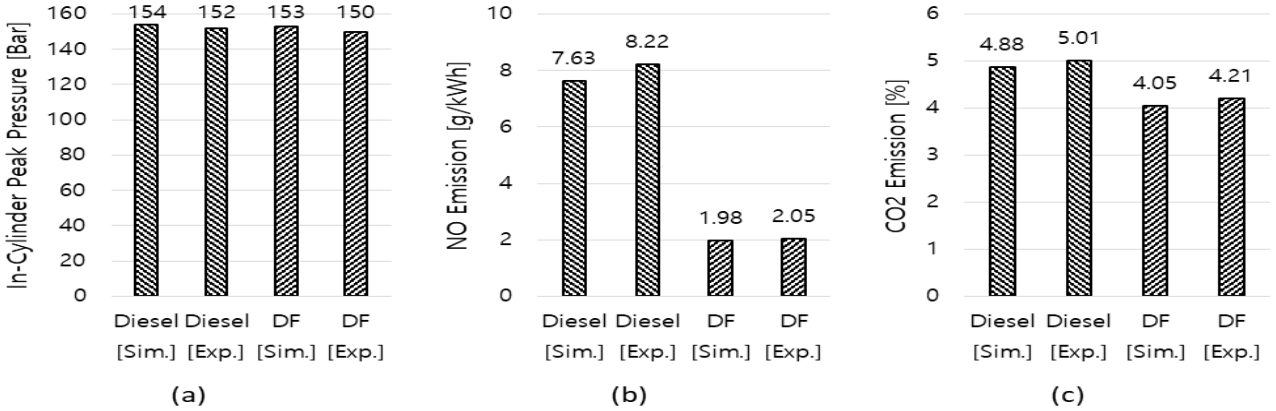

Figure 3. Comparison between simulation and experimental result: (a) In-Cylinder peak pressure, (b) NO emission and (c) CO_2 emission.

It is obvious that the simulation and experimental results are in good agreement. In the diesel mode, the deviations between the simulated and experimental NO and CO_2 emissions were 7.77% and 2.66%, respectively. Whereas, the deviation between the simulated and experimental peak pressures was only 2.56%. In the DF mode, the deviation between the experimental and simulated peak pressures was only

1.96%, while the deviations between the experimental and simulated NO and CO_2 emissions were 3.53% and 3.8%, respectively. After the CFD models were validated, they were suitable and applied to model the combustion process and emission formations occurring inside the cylinder of the engine for all simulation cases in this study.

F. Mesh Independence Analysis

The final CFD result accuracy is greatly influenced by the mesh quality (or mesh resolutions). On another hand, mesh resolutions affect calculation time. Generally, a finer mesh may give a better mesh quality leading to a higher CFD result accuracy. However, it also prolongs calculation time. Thus, to ensure the final CFD result accuracy and reasonableness of the calculation time, a mesh independence analysis was conducted by performing three simulations with various mesh resolutions, including a coarse, medium, and fine mesh.

Table V lists the mesh properties and calculation time of these three various mesh resolutions.

TABLE V. MESH PROPERTIES AND CALCULATION TIME.

Mesh Resolution	**Mesh 1 - Coarse**	**Mesh 2 - Medium**	**Mesh 3 - Fine**
No. of faces of the 2D mesh at the TDC	12,949	17,715	39,307
No. of cells of the 3D mesh	586,796	882,620	1,593,732
Calculation times	24 h	36 h	92 h

Figure 4 presents the final CFD results for the three various mesh resolutions. As shown in the figure, the final CFD results were no longer dependent on the mesh resolution. Therefore, all these meshes can technically be used for simulations to obtain highly accurate and mesh-independent CFD results. However, mesh 2 was selected to perform simulations in the present study because it gave accurate results in a reasonable time. It also has an appropriate resolution for a good contour analysis.

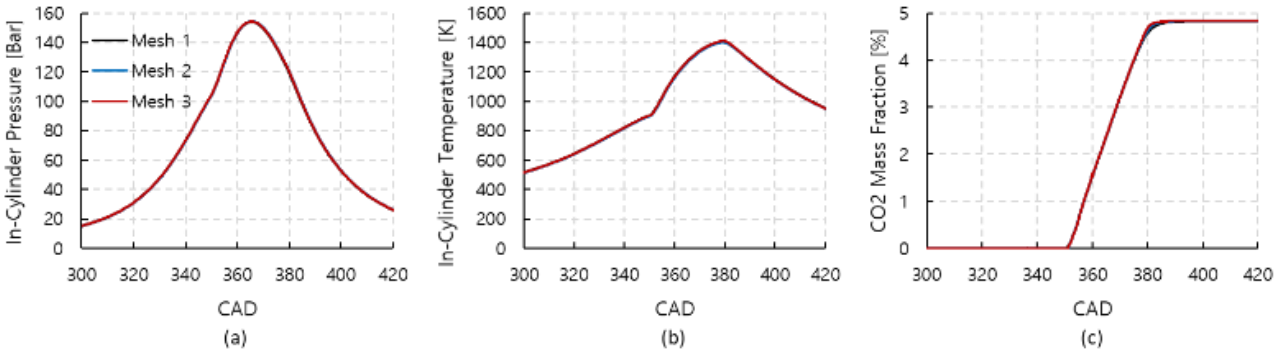

Figure 4. Mesh independence analysis results: (a) In-Cylinder pressure, (b) In-ylinder temperature and (c) CO_2 emission.

III. SIMULATION RESULTS

A. In-Cylinder Pressure

The pressure and rate of heat release (RoHR) inside the engine cylinder are shown in figure 5. The simulation result showed a little lower in-cylinder peak pressure in the DF modes than in the diesel mode. The lower peak pressure in the DF modes is because of the lower pilot diesel fuel which was injected to provide the ignition source for the NG. As known, the combustion process of ICEs is divided into four stages: (1) ignition delay (ID); (2) premixed combustion; (3) diffusion combustion; and (4) late stage of combustion. In these four stages, stages 1 and 2 play a critical role in the increase rate and thus peak pressure in the cylinder. The longer the ID and premixed combustion, the higher the pressure rise rate and peak pressure. In the DF modes, only 5% of diesel oil was used for ignition, so the ID and premixed combustion stages were very short. This reduced the in-cylinder peak pressure.

Figure 6 presents the in-cylinder peak pressure in all operating modes. The result showed a reduction in peak pressure as the injector SA increased from 145 to 160°. This may be because of the increase in the fuel-air mixing quality when the SA increases. As the SA increases the interaction area between injected fuel and air increases accordingly resulting in an increase in the fuel-air mixing quality. An increase in the mixing quality reduced the ID and thus peak pressure inside the engine cylinder when the fuel burnt.

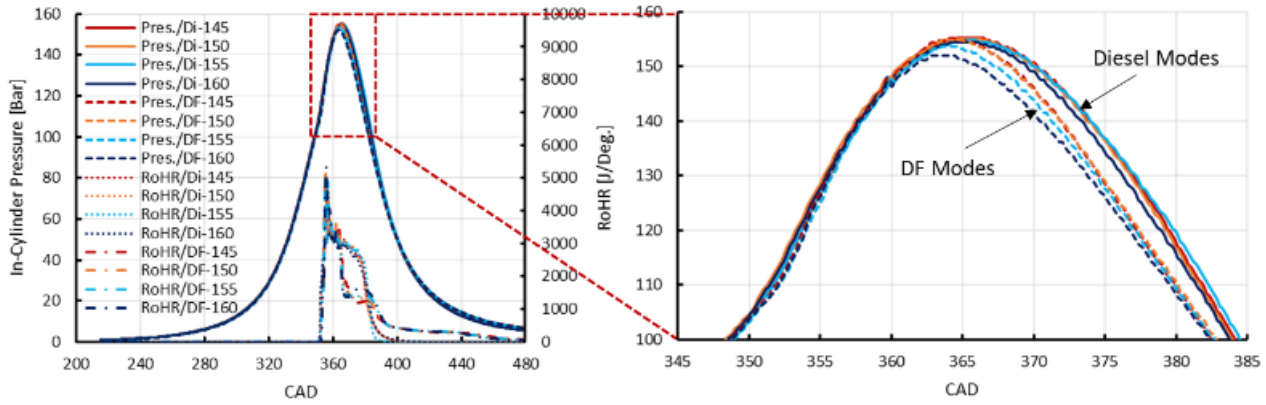

Figure 5. In-Cylinder peak pressure and RoHR in all operating cases.

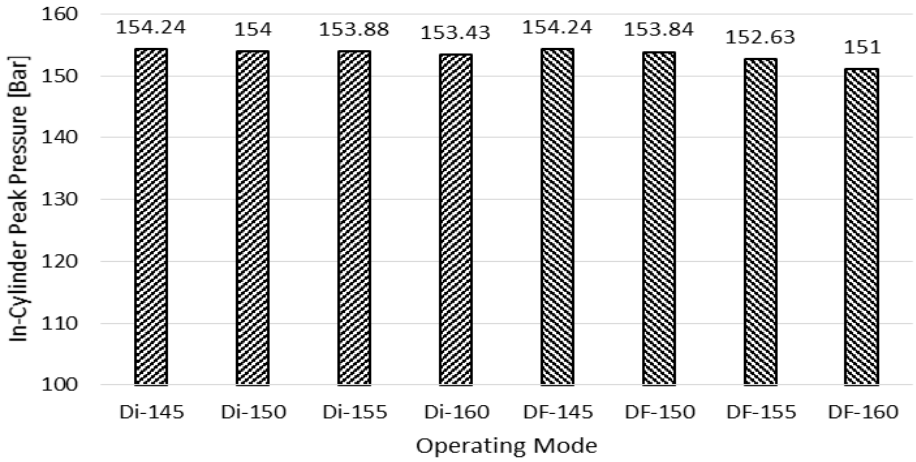

Figure 6. In-Cylinder peak pressure in all operating modes.

B. In-Cylinder Temperature

The temperature inside the engine cylinder is shown in figure 7. The simulation result showed lower in-cylinder peak temperature in the DF modes than in the diesel mode. However, the in-cylinder temperature during the late stage of combustion in the DF modes was higher than that in the diesel mode. The lower peak temperature and higher temperature during the late stage combustion are characteristic features of port-injection premixed combustion compared to the direct-injection combustion. In the port-injection method, fuels are injected into the intake port of the engine during the intake stroke. During the compression stroke, both fuel and charge air are compressed together. Therefore, there is enough time for the fuel and charge air to mix with each other to form a premixed mixture prior to an ignition source being supplied for ignition. Due to the fuel-air mixture being perfectly prepared for combustion, the combustion inside the cylinder using the port-injection method occurs more uniformly than in the direct-injection method.

The more uniform temperature distribution within the engine combustion chamber reduced peak temperature as can be seen in figure 7.

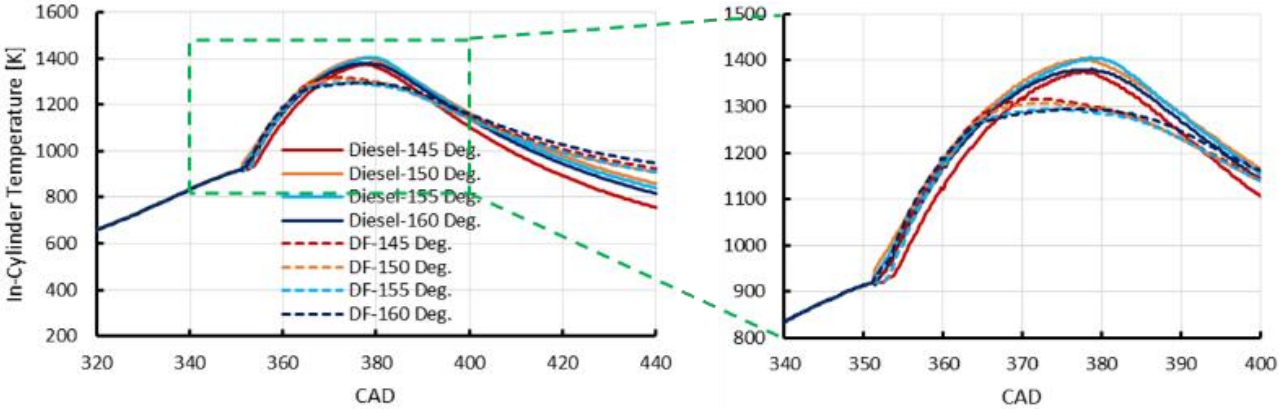

Figure 7. In-Cylinder temperature in all operating modes.

Figure 8 presents the temperature contour inside the engine cylinder at the top dead center (TDC) in all simulation cases. As we can see in the figure, the SA of 155^{o} and 150^{o} produced the highest local peak temperatures in the diesel and DF mode, respectively.

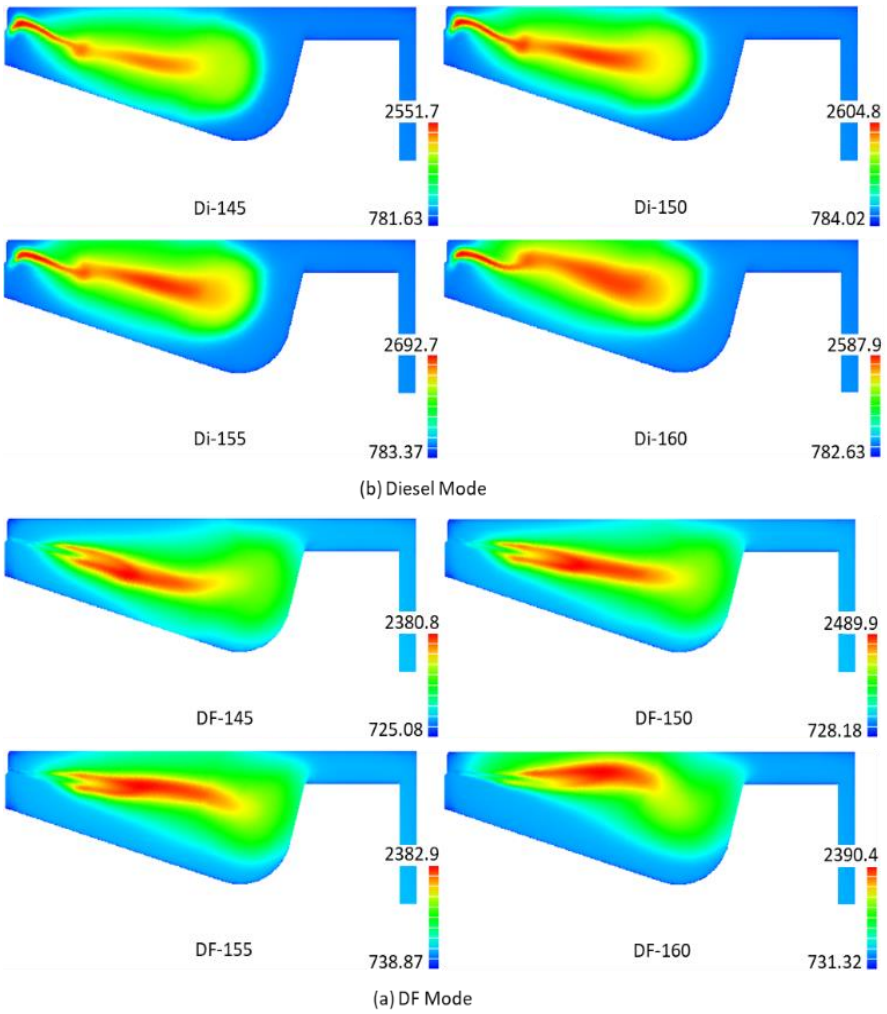

Figure 8. Temperature contour at the TDC in all simulation cases

C. NO emission

Figure 9 presents the NO emission in all simulation cases. The results showed a significant reduction in NO emission in the DF modes compared to the diesel modes. The DF mode helped to reduce NO emission by around 71% compared to the diesel mode.

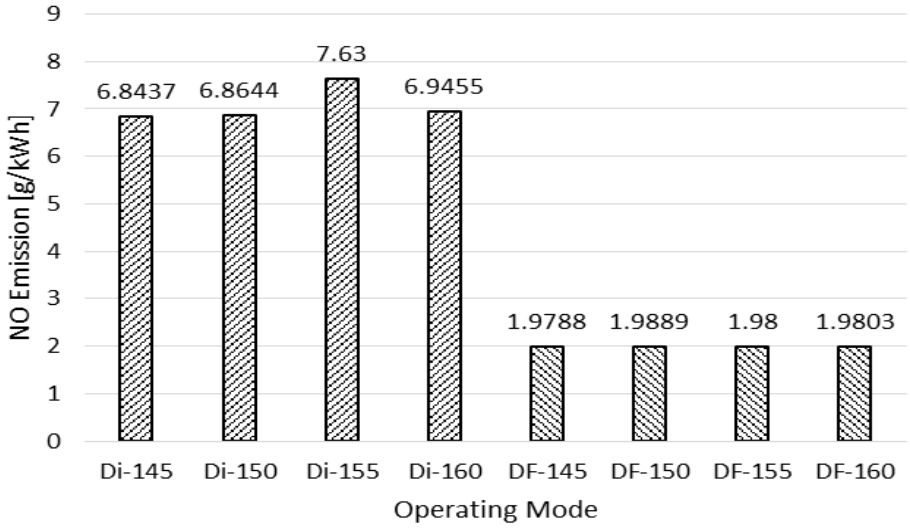

Figure 9. NO emission in all simulation cases.

NO occupies more than 90% of NOx emissions generated from ICEs. Chemically, two chemical mechanisms need to be considered when analyzing NO emissions: thermal NO mechanism (Zeldovich mechanism) and prompt NO mechanism (Fenimore mechanism) [18]. However, in ICEs, only the thermal NO mechanism must be considered when analyzing NO and thus NOx emissions. Therefore, this study used the extended Zelodovich mechanism to model NO formation. According to the thermal NO mechanism, NO formation is strongly influenced by the local in-cylinder peak temperature, oxygen (O_2) concentration, and resident time. NO is mainly formed in regions where the temperature is above 1800 K in the cylinder. The formation rate increases dramatically with the increase of local in-cylinder peak temperature [14], [18], [19].

In the DF modes, as showed in figure 8, the peak temperature was significantly reduced compared to the diesel mode. This led to a reduction in NO emission as shown in figure 9. The SA of 155^o and 150^o respectively produced the highest peak temperature in the diesel and DF mode, resulting in the highest NO emission in these corresponding modes. On the other hand, the SA of 145^o produced the lowest NO emission in both the diesel and DF modes. This is because this SA generated the lowest peak temperature in both the diesel and DF modes.

In addition, the gaseous fuel was injected into the intake port in the DF modes to mix with fresh air generating a homogeneous premixed mixture prior to be supplied to the engine cylinder. These results in a significant reduction in the local O_2 concentration in the engine cylinder. This contributes to the reduction in the NO emissions when burning gaseous compared to diesel only. In conclusion, the SA of 145^o is the optimal value for reducing NO emission in both the diesel and DF mode.

D. Soot

Soot is the main component of particulate matter (PM) emissions [20]-[23]. Under high fuel-air equivalence ratios (fuel-rich) and high-temperature conditions, which are typically found in DI diesel engines, hydrocarbon fuels have a very strong tendency to form carbonaceous particles, i.e., soot. Under the normal running condition of engines, most soot formed in the early stages of combustion is burnt owing to oxidation with O_2 in oxygen-rich regions inside the engine cylinder in the later stage of combustion. In ICEs, the completeness of the soot oxidation process and thus the final amount of soot actually determine their PM characteristics [17]. The local fuel-air equivalence, temperature, pressure, and residence time play the most important role in the soot formation of DI engines [17]. Soot particles are formed very early in the diffusion stage of combustions owing to the dissociation of fuels under high equivalence ratio and temperature conditions.

Figure 10 presents the soot emission in all simulation cases. The result showed a significant reduction in soot in the DF modes compared to the diesel modes. The soot emission in the DF modes was almost zero. This is because the fuel-air mixing quality between the supplied fuel and charge air in the DF modes (using the port injection method) was significantly higher than that in the diesel mode (using the direct injection method). A higher fuel-air mixing quality led to significant reductions in the local fuel-air equivalence ratio in the DF modes. This reduced soot formation in the DF mode. Additionally, because CH_4, the simplest and cleanest hydrocarbon fuel, does not contain C-C bonds in its chemical structure, and contains no aromatics and sulfur, it tends to minimally produce soot emissions compared to other hydrocarbon fuels [1], [24]. The reduction tendencies in soot formation in DF modes using CH_4 as the primary fuel compared to the diesel mode using diesel oil had also been reported in previous studies [8], [9].

In both the diesel and DF modes, the SA of 150^o produced the lowest soot emission. This is the recommended SA for the injector of this engine to reduce soot emission. It helped to reduce 56% and 17% soot in the diesel and DF modes, respectively.

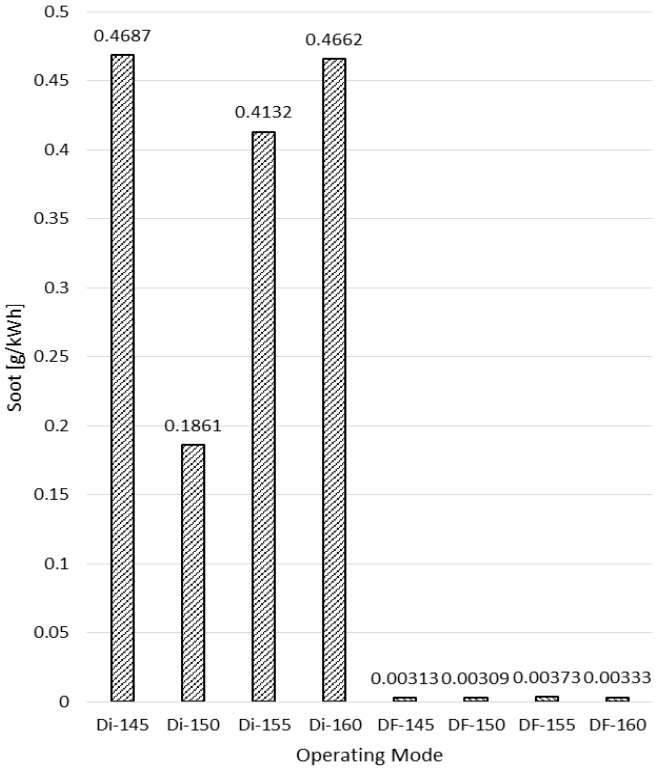

Figure 10. Soot emission in all simulation cases.

E. CO_2 emission

Figure 11 presents the CO_2 emission in all simulation cases. The result showed a considerable reduction in CO_2 emission in the DF modes compared to the diesel modes. The DF modes helped to reduce CO_2 emission by around 20% compared to the diesel modes. As is widely known, carbon dioxide (CO_2) is carbon-based emissions. Its formation is directly dependent on the number of carbon (C) atoms contained in the fuel. Moreover, its formation is significantly influenced by the combustion quality inside the engine cylinder. CO_2 is a product of the complete combustion of hydrocarbon fuels. In ICEs, hydrocarbon fuel is firstly oxidized by O_2 contained in the charge air to form CO during the combustion. CO is then oxidized to form CO_2 sequentially if there is still enough O_2 in high-temperature conditions in the engine cylinder. In this study, compared to the diesel modes, the DF modes reduced CO_2 emissions due to the better fuel-air mixing quality of the port injection compared to the direct injection method, and the cleaner characteristics and fewer C atoms of NG compared to the diesel oil. The reduction tendencies of CO_2 emissions in DF modes when using NG as the primary fuel compared to the diesel mode had also been reported in many previous studies [8], [9]. In both the diesel and DF modes, the SA of 150^o produced the lowest CO_2 emission. This is the recommended SA for the injector of this engine to reduce CO_2 emission. It helped to reduce 0.77% and 0.31% CO_2 emissions in the diesel and DF modes, respectively.

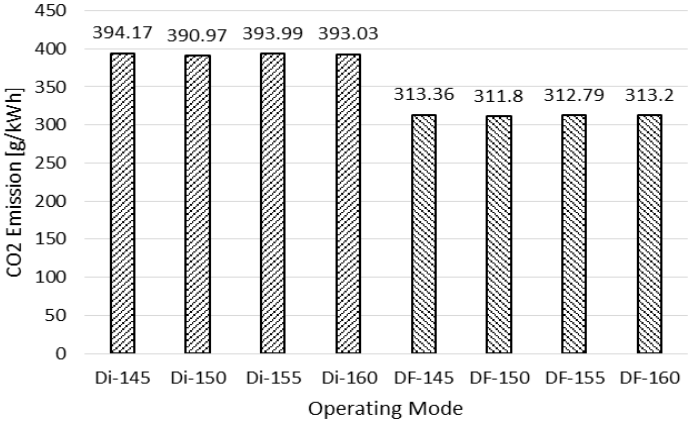

Figure 11. CO_2 emission in all simulation cases.

IV. CONCLUSION

This work numerically investigated the effect of the injector SA on the combustion process and emission characteristics of a 4-stroke NG-Diesel DF marine engine aiming to find out the optimal SA for the injector of the engine to reduce exhaust gas emission without using any post-treatment devices.

The major results of the study are listed as follows:

- The simulation result showed lower in-cylinder peak temperature in the DF modes than in the diesel mode due to the more uniform temperature distribution within the engine combustion chamber.
- The DF mode helped to reduce NO emission by around 71% compared to the diesel mode. The SA of 145 ^{o} is the optimal value for reducing NO emission in both the diesel and DF mode.
- The result showed a significant reduction in soot in the DF modes compared to the diesel modes. The soot emission in the DF modes was almost zero. In both the diesel and DF modes, the SA of 150^{o} produced the lowest soot emission. This is the recommended SA for the injector of this engine to reduce soot emission. It helped to reduce 56% and 17% soot in the diesel and DF modes, respectively.
- The result showed a considerable reduction in CO_2 emission in the DF modes compared to the diesel modes. The DF modes helped to reduce CO_2 emission by around 20% compared to the diesel modes. In both the diesel and DF modes, the SA of 150^{o} produced the lowest CO_2 emission. This is the recommended SA for the injector of this engine to reduce CO_2 emission.

Based on the above conclusions, it is highly recommended to use a SA of 145^{o} or 150^{o} for the fuel injector to reduce NO or soot and CO_2 emissions, respectively, depending on which emission regulations need to be met.

REFERENCES

[1] H. Thomson, J. J. Corbett, J. J. Winebrake, "Natural gas as a marine fuel," Energy Policy, vol. 87, pp. 153–167, 2015. DOI:10.1016/j.enpol.2015.08.027.

[2] Z. Wang, S. Zhou, Y. Feng, Y. Zhu, "EGR modeling and fuzzy evaluation of Low-Speed Two-Stroke marine diesel engines," Science of The Total Environment, vol. 706, 2020. DOI:10.1016/j. scitotenv.2019.135444.

[3] L. Bilgili, "Life cycle comparison of marine fuels for IMO 2020 Sulphur Cap," Science of The Total Environment, vol. 774, 2021. DOI:10.1016/j.sci totenv.2021.145719.

[4] UNCTAD, "COVID-19 and maritime transport: Impact and responses," Transport and Trade Facilitation Series No. 15, NY, USA: Routledge, 2020. Available: https://unctad.org/webflyer/covid-19-and-maritime-transport-impact-and-responses. Accessed on: 20/6/2022.

[5] J.Shu et al, "Effects of injector spray angle on combustion and emissions characteristics of a natural gas (NG)-diesel dual fuel engine based on CFD coupled with reduced chemical kinetic model," Applied Energy, vol. 233-234, pp. 182–195, 2019.

[6] N.R. Banapurmath, et al., "Combustion characteristics of a four-stroke CI engine operated on Honge and Jatropha oil methyl ester–ethanol blends when directly injected and dual fuelled with CNG induction," International Journal of Sustainable Engineering, vol. 4, no. 2, pp. 145–152, 2011. DOI:10.1080/19397038. 2010.540680.

[7] G. Decan, T. Lucchini, G. D'Errico, S. Verhelst, "A novel technique for detailed and time-efficient combustion modeling of fumigated dual-fuel internal combustion engines," Applied Thermal Engineering, vol. 174, 2020. DOI: 10.1016/j.applthermaleng. 2020.115224.

[8] V. C. Pham, et al., "A numerical study on the combustion process and emission characteristics of a natural gas-diesel dual-fuel marine engine at full load," Energies, vol. 14, no. 5, 2021.

[9] V. C. Pham, et al., "Effects of various fuels on combustion and emission characteristics of a four-stroke dual-fuel marine engine," J. Mar. Sci. Eng., vol. 9, no. 10, 2021. DOI:10.3390/jmse9101072.

[10] S. Wei, K. Ji, X. Leng, F. Wang, X. Liu, "Numerical simulation on effects of spray angle in a swirl chamber combustion sys-tem of DI (direct injection) diesel engines," Energy, vol. 75, pp. 289–294, 2014.

[11] H. J. Kim, S. H. Park, C. S. Lee, "Impact of fuel spray angles and injection timing on the combustion and emission characteris-tics of a high-speed diesel engine," Energy, vol. 107, pp. 572–579, 2016. DOI:10.1016/j.energy.2016.04.035.

[12] L. Eder, M. Ban, G. Pirker, M. Vujanovic, P. Priesching, A. Wimmer, "Development and validation of 3D-CFD injection and combustion models for dual fuel combustion in diesel ignited large gas engines," Energies, vol. 11, no. 3, 2018. DOI:10.3390/en11030 643.

[13] P. A. Durbin, "Near-wall turbulence closure modeling without "damping functions". Theor. Comput. Fluid

Dyn., vol. 3, pp. 1–13, 1991. DOI: 10.1007/BF00271513.

[14] S. Candel, D. Veynante, F. Lacas, E. Maistret, N. Darabiha, T. Poinsot, "Coherent flamelet model: Applications and current extensions," Recent Advances in Combustion Modelling, Advances in Mathematics for Applied Sciences, pp. 19–64, 1990. DOI:10.1142/9789814293778_0002.

[15] Austria AVL List GmbH, "Combustion Module User Manual," AVL FIRE® R2018a, Graz, Austria, 2018.

[16] AVL List GmbH, "Spray Module User Manual," AVL FIRE® R2018a, Graz, Austria, 2018.

[17] AVL List GmbH, "Emission Module User Manual," AVL FIRE® R2018a, Graz, Austria, 2018.

[18] L. Wei, P. Geng, "A review on natural gas/diesel dual fuel combustion, emissions and performance," Fuel Processing Technology, vol. 142, pp. 264–278, 2016. DOI:10.1016/j.fuproc.2015.09.018.

[19] J. B. Heywood, "Internal Combustion Engine Fundamentals," NY, USA: McGraw-Hill Education, 1998.

[20] M. M. Maricq, R. E. Chase, N. Xu, P. M. Laing, "The effects of the catalytic converter and fuel sulfur level on motor vehicle particulate matter emissions: Light duty diesel vehicles," Environmental Science & Technology, vol. 36, no. 2, pp. 283–289, 2002. DOI:10.1021/es010962l.

[21] R. T. Burnett, S. Cakmak, J. R. Brook, D. Krewski, "The role of particulate size and chemistry in the association between summertime ambient air pollution and hospitalization for cardiorespiratory diseases," Environmental Health Perspectives, vol. 105, no. 6, pp. 614–620. DOI:10.1289/ehp.97105614.

[22] D. B. Kittelson, W. F. Watts, J. P. Johnson, "On-road and laboratory evaluation of combustion aerosols—Part1: Summary of diesel engine results," Journal of Aerosol Science, vol. 37, no. 8, pp. 913–930, 2006. DOI:10.1016/j.jaerosci.2005.08.005.

[23] Rounce, P.; Tsolakis, A.; York, A.P.E, "Speciation of particulate matter and hydrocarbon emissions from biodiesel combustion and its reduction by after treatment," Fuel, vol. 96, no. 1, pp. 90–99, 2012. DOI:10.1016/j.fuel.2011.12.071.

[24] Q. Zhang, M. Li, S. Shao, "Combustion process and emissions of a heavy-duty engine fueled with directly injected natural gas and pilot diesel," **Applied Energy** vol, 157, pp. 217–228, 2015. DOI:10.1016/j.apenergy.2015.08.021.